Probing Reactivity of Gold Atoms with Acetylene and Ethylene with VUV Photoionization Mass Spectrometry and ab initio Studies

Ricardo B. Metz,[a] Gokhan Altinay,[a] Oleg Kostko[b] and Musahid Ahmed[b]*

a) Department of Chemistry, University of Massachusetts Amherst, Amherst, MA 01003 USA

b) Chemical Sciences Division, Lawrence Berkeley National Laboratory, Berkeley, California 94720 USA

Abstract

Reaction of gold atoms with acetylene and ethylene in a laser ablation source produces a number of gold-containing species. Their photoionization efficiency (PIE) curves are measured using tunable vacuum ultraviolet (VUV) radiation at the Advanced Light Source. Their structures are assigned by comparing the experimental ionization energies and PIE curves to those of potential isomers calculated at the CAM-B3LYP/aug-cc-pVTZ level. For smaller molecules, the contribution of ionization to excited electronic states of the cation is also included using photoionization cross sections calculated using *ePolyScat*. Reaction with acetylene produces adducts $Au(C_2H_2)$ and $Au(C_2H_2)_2$, as well as $HAu(C_4H_2)$. Reaction with ethylene leads to adducts $Au(C_2H_4)$, $Au(C_2H_4)_2$, an adduct with gold dimer, $Au_2(C_2H_4)$, as well as the gold hydrides AuH, $HAu(C_2H_4)$ and $HAu(C_4H_4)$. [Au,C4,H7] is also observed and it likely corresponds to a gold alkyl, $H_2C{=}C(H){-}Au(C_2H_4)$. Reactions leading to production of odd-hydrogen species are endothermic and are likely due to translationally or electronically excited gold atoms. These measurements provide the first directly measured ionization energy for gold hydride, IE(AuH) = 10.25 ± 0.05 eV. Combining this value with the dissociation energy of AuH^+ gives a dissociation energy $D_0(AuH)$ = 3.15 ± 0.12 eV. Several other ionization energies are measured: IE($Au_2(C_2H_4)$) = 8.42 ± 0.05 eV, IE($HAu(C_2H_4)$) = 9.35 ± 0.05 eV, IE($HAu(C_4H_2)$) = 8.8 ± 0.1 eV and IE($HAu(C_4H_4)$) = 8.8 ± 0.1 eV.

* Corresponding author. E-mail address: rbmetz@chem.umass.edu

1. Introduction

Although it had long been considered relatively inert, over the last two decades there has been a huge increase in the use of gold in homogeneous and heterogeneous catalysis, frequently involving alkenes and alkynes as substrates.[1-6] A key aspect to many of these reactions is the ability of gold to activate π bonds for subsequent nucleophilic addition.[5, 7-9] Gas-phase studies can elucidate the intrinsic interactions of gold-containing species, and there have been extensive investigations of the reactivity and bonding of bare and ligated gold complexes, particularly cationic species.[10-14] Complexes of Au and Au^+ with acetylene and ethylene have been studied extensively, both experimentally and computationally. There is much less known about the interactions of gold hydrides with alkenes and alkynes, although these species have been proposed as reaction intermediates in homogeneous catalysis.[2, 15-16]

Most reaction studies of neutral metal atoms monitor the loss of the atom, so the products aren't known.[14] Studies of reactions of metal cations typically also measure product masses, but isomeric products aren't identified. In the present study gold-containing compounds are produced by reacting laser-ablated gold atoms with ethylene and acetylene. The masses of reaction products are determined by photoionization and mass spectrometry. In addition, the use of tunable VUV from a synchrotron for ionization allows us to measure the photoionization efficiency (PIE) as a function of photon energy. This often permits differentiation between possible isomers based on differences in their ionization energy and calculated PIEs. This feature has been demonstrated in numerous studies of reactions of main-group atoms and transition metals carried out at the Chemical Dynamics Beamline with tunable VUV radiation.[17-24]

The development of efficient computational methods to accurately treat relativistic effects is an active area of theory. Relativistic effects are extremely important in the chemistry of gold,[25-26] so gold-containing compounds are often used to benchmark new computational approaches.[26-28] Thus, an added motivation for these experiments is to provide accurate ionization energies that can be used to evaluate electronic structure methods.

2. Experimental and Computational Methods

The photoionization experiments were carried out at the Chemical Dynamics Beamline at the Advanced Light Source (ALS) at Lawrence Berkeley National Laboratory.[17-20] As in our study of the intermediates and products of reactions of platinum with methane[23] the neutral

molecules of interest are produced via pulsed laser ablation and subsequent reactions and are characterized by measuring their mass-analyzed photoionization efficiency curves (PIE).

Laser ablation (532 nm second harmonic of a Nd:YAG laser operating at 50 Hz repetition rate) of a brass rod plated with gold (Fountain Plating, Springfield, MA, 99.97% pure) produces gold atoms that then cluster and/or react with the gaseous hydrocarbon of interest (methane, ethene or acetylene) introduced via a pulsed piezoelectric valve. The molecules cool in the supersonic expansion. The resulting molecular beam is skimmed and the neutral molecules are irradiated by VUV light. The beamline provides tunable VUV light with photon energies of 8-16 eV, pulsed at a repetition rate of 500 MHz. The VUV line width is determined by the slit width on a 3 meter monochromator. Due to the low signal levels, all data was obtained using 1300 μm slits, which corresponds to FWHM of ~40 meV at 9 eV and ~50 meV at 10 eV. A pulsed voltage extracts the photo-ions into a reflectron time-of-flight mass spectrometer where they are detected and tallied by a dual micro channel plate detector and fast counter. Ion masses are determined from their flight times. Mass spectra are measured at each VUV photon energy, summing the signal over 10000 to 20000 laser shots at each energy. PIEs are measured by integrating the area under the peak in the mass spectrum corresponding to each ion of interest, normalized to VUV flux measured using a silicon photodiode, at each VUV energy. Error bars in the PIE are based on counting statistics.

Calculations were carried out to identify possible structures for the neutral molecules observed, their energetics, ionization energies and, in most cases, to simulate their PIEs. The electronic structure calculations were carried out using *Gaussian09*,[29] employing the CAM-B3LYP functional with the aug-cc-pVTZ-PP relativistic effective core potential and basis set[30] for gold and aug-cc-pVTZ basis set for carbon and hydrogen. This functional and basis set give ionization energies in excellent agreement with experiment for species involved in the Pt + CH_4 reaction[23] and agree with benchmark CCSD(T) calculations for energetics of gold atom-catalyzed oxidation of CO.[31] Harmonic frequencies were calculated at each stationary point to ensure that it is a minimum and are not scaled. All reported energies include zero-point energy. Calculations use the ultrafine integration grid. Calculated and measured ionization energies are summarized in Table 1 and dissociation energies are collected in Table 2. Energies and calculated structures of all species discussed, including Au(C_2H_2) and singlet and triplet states of Au^+(C_2H_2), are in Table S1.

In most cases, PIE curves are calculated by computing the geometries and vibrations of the neutral and cation, and calculating Franck-Condon factors (FCFs) for each vibration. The products of the Franck-Condon factors are then integrated and convolved with a Gaussian function with the VUV linewidth.[23, 32] If the neutral and cation have the same symmetry, FCFs are calculated in *Gaussian09* using harmonic oscillators. If one is of lower symmetry, then the potential is scanned along the vibration which breaks the symmetry, and FCFs for that vibration are calculated numerically. Similarly, if there is a large geometry change in a coordinate on ionization, the potential is scanned and, if it is not harmonic, FCFs are calculated numerically. The ionization energy is determined by shifting the energy origin of the simulation until it provides the best match to the measured PIE spectrum. In some cases, the PIE extends to sufficiently high energies that photoionization can access excited electronic states of the cation. To estimate the relative contributions of the ground and excited states to the PIE as a function of photon energy, we calculate the photoionization cross section using *ePolyScat* (version E),[33] developed by the groups of Lucchese and Gianturco.[34-36] Details of the procedure for the photoionization cross section calculations are in the SI.

3. Results and Discussion

A. Reaction Products

A small amount of AuH is observed from reaction of laser-ablated gold atoms with methane. Reaction with acetylene produces molecules with even numbers of hydrogens, [Au,C2,H2], [Au,C4,H4] and [Au2,C2,H2], as well as one with odd numbers of hydrogens: [Au,C4,H3], as shown in Figure 1. Similarly, reaction with ethylene yields the even-hydrogen complexes [Au,C2,H4], [Au,C4,H8] and [Au2,C2,H4] and odd-hydrogen complexes AuH, [Au,C2,H5], [Au,C4,H5] and [Au,C4,H7]. Photoionization efficiency curves (PIEs) are measured for each molecule. The structure of the isomer produced by the reaction is determined by comparing the measured ionization energy and PIE to those calculated for candidate structures. The even- and odd-hydrogen complexes will be discussed separately.

B. Even-Hydrogen Complexes

All of the even-hydrogen products are non-covalent complexes formed by clustering of gold or gold dimer to ethylene or acetylene. The PIE of [Au,C2,H2], Figure 2, shows a small

amount of ionization at the lowest photon energy measured, 8 eV, with the photoionization cross section increasing gradually and steadily above ~9.5 eV. Non-covalent complexes of Au with alkanes are expected to have ionization energies much lower than those of gold atom (9.226 eV),[37] as the charge leads Au^+ to bind more strongly to alkanes than Au^0. Also, the PIE typically increases only gradually with energy, as the neutral and cation have substantially different geometries, as shown in Figure 3. The calculations predict that the ionization energy of $Au(C_2H_2)$ is 7.06 eV. This low ionization energy is due to the large difference between the Au^+-C_2H_2 and Au-C_2H_2 bond dissociation energies, 2.35 eV and 0.16 eV, respectively. If there is no geometry change upon ionization, the calculations predict that the photoionization cross section rises sharply at the ionization energy and then slowly decreases with increasing photon energy. A change in geometry upon ionization leads to a more gradual onset. These features are clearly observed in the PIEs of $Au(C_2H_2)$, Figure 2 and $Au(C_2H_4)$, Figure S2. The observed increase in the PIE at higher energy is due to ionization to excited electronic states of $Au^+(C_2H_2)$, with a calculated onset of 9.82 eV to formation of the lowest triplet state. Several additional triplet states and excited singlet states are predicted to become accessible at photon energies of 10.2 to 11 eV, as shown in Figure 2. Surprisingly, the vinylindene complex $AuCCH_2$ is calculated to lie only 0.09 eV above $Au(C_2H_2)$. Its ionization energy to $AuCCH_2^+$ is predicted to be quite low, 7.43 eV. Although the experiment offers no evidence for or against its presence, there is likely to be a significant barrier to its formation from Au + C_2H_2. Matrix isolation studies of gold atoms co-deposited with acetylene observe $Au(C_2H_2)$ π-complexes and structures analogous to vinyl radical, with gold substituted for one of the hydrogen atoms at ~4 K, and $AuCCH_2$ at 77 K.[38-40] Our calculated Au^+-C_2H_2 dissociation energy agrees with the value of 2.42 eV obtained by Kang et al.[9] at the CCSD(T) level, extrapolated to the complete basis set limit. Several DFT calculations also predict similar bond dissociation energies.[9, 41] The calculations predict that the C-C bond lengthens by 0.014 Å when C_2H_2 binds to Au; this extension is greater for the Au^+ complex, 0.035 Å. Ward et al.[42] measured vibrational spectra of $Au^+(C_2H_2)_n$ complexes in the C-H stretching region, using IR photodissociation of the argon-tagged complexes for the n=1 and 2 clusters. They find that binding to the metal cation results in a red shift of ~115 cm^{-1} in the acetylene C-H stretches for n=1 and ~100 cm^{-1} for n=2. This red shift is consistent with the classic Dewar-Chatt-Duncanson model of metal coordination.[43-44] The PIE of [Au,C4,H4] from Au + C_2H_2 is shown in Figure S1. The ionization energy is below 8 eV, and the photoionization

yield increases steadily starting at ~8.5 eV. This is consistent with it being due to $Au(C_2H_2)_2$. There is a small amount of [Au2,C2,H2] formed by reaction of gold with C_2H_2. It is likely $Au_2(C_2H_2)$. However, the signal is too low to measure an accurate PIE curve.

Interaction of laser-ablated gold atoms with ethylene produces [Au,C2,H4], [Au,C4,H8] and [Au2,C2,H4]. The PIE of [Au,C2,H4], Figure S2, shows substantial signal at the lowest photon energy, 8 eV, is flat until ~9.25 eV, then increases gradually. This is consistent with $Au(C_2H_4)$ (Fig. 3), which is calculated to have an ionization energy of 6.86 eV. Ionization to the lowest excited electronic state, the triplet, is calculated to occur at 9.63 eV. The covalent $AuCHCH_3$ isomer is calculated to lie 0.58 eV above $Au(C_2H_4)$, so it is not likely to be formed. McIntosh and Ozin measured the vibrational and electronic spectra of $Au(C_2H_4)$ in an argon matrix.[45] This study and a subsequent ESR/matrix isolation study by Kasai[38] only observe the $Au(C_2H_4)$ π complex. There is about an order of magnitude more $Au^+(C_2H_4)$ signal from Au + C_2H_4 than $Au^+(C_2H_2)$ from Au + C_2H_2. The calculations predict similar photoionization cross sections for the corresponding neutrals, so the increased signal is likely due to the higher calculated bond dissociation energy of Au to C_2H_4, 0.24 eV, than C_2H_2, 0.16 eV.

Our calculations predict that the low IE of $Au(C_2H_4)$ is due to the very high bond dissociation energy of Au^+-C_2H_4, 2.62 eV. There are numerous calculations of the $Au^+(C_2H_4)$ bond dissociation energy (BDE). Particularly noteworthy are an atoms-in-molecules bonding analysis study by Hertwig et al.[46] who determined that it should be classified as a metallocyclopropane, and an energy decomposition analysis of the bonding by Nechaev et al.[47] These studies calculated BDEs of 2.97 and 3.16 eV at the B3LYP/RECP and BP86/TZP levels, respectively. Calculations at the CCSD(T) level with an extrapolation to the complete basis set limit by Kang et al.[9] predict a BDE of 2.77 eV; this study also calculated BDEs with several density functionals. Li et al. carried out a relativistic CCSD(T) calculation with a large basis set, obtaining a BDE of 2.70 eV.[48] Experimentally, Bowers and coworkers[49] used temperature-dependent equilibrium measurements to determine the bond dissociation energies of Au_x^+ (x=1, 3-9) with C_2H_4. They obtain a bond dissociation enthalpy 2.60 eV ≤ $\Delta H(Au^+$-$C_2H_4) \leq 3.09 \pm 0.11$ eV. Schröder et al. determined a lower limit of BDE ≥ 2.82 eV based on the observed reaction of Au^+ with iodobenzene to give AuI^+ and reaction of ethene with AuI^+ to give $Au^+(C_2H_4)$.[10, 50] Stringer et al. observe an onset of 28,800 cm^{-1} (3.57 eV) for production of Au^+ from photodissociation of $Au^+(C_2H_4)$, providing an upper limit to the BDE.[51-52] Based on the high-

level CCSD(T) calculations, the BDE is likely to be very close to the experimental lower limit of Schröder et al. Both $Au(C_2H_4)$ and $Au^+(C_2H_4)$ are calculated to have C_{2v} symmetry. The Au-C bond lengths are substantially shorter in the cation, and the C-C bond length is significantly longer. Binding to Au^+ is predicted to lengthen the C-C bond in C_2H_4 by 0.067 Å, further supporting its assignment as a metallocyclopropane.

Gold atoms and cations interact slightly more strongly with C_2H_4 than with C_2H_2. This is evident in the calculated bond dissociation energies, which are 0.08 eV and 0.27 eV higher for the neutrals and cations, respectively (Table 2). This is consistent with previous DFT and CCSD(T) calculations.[9, 53] This effect is not unique to gold – it is also calculated to occur in complexes of first-row transition metal cations, for which Sodupe et al. attributed the higher bond dissociation energy for C_2H_4 to be due to its higher polarizability, particularly along the metal-ligand axis.[54] The PIE of [Au,C4,H8], also shown in Figure S2, is similar to that of $Au(C_2H_4)$ and is consistent with formation of $Au(C_2H_4)_2$. Again, the ionization energy is below 8 eV, and the cross section increases above 8.8 eV.

Unlike the other even-hydrogen species, we do observe the photoionization onset for $Au_2(C_2H_4)$, as shown in Figure 4. The ionization energy of $Au_2(C_2H_4)$ is calculated to be 8.16 eV. We determine its ionization energy by simulating the PIE curve, and shifting it until it matches the data. This gives $IE(Au_2(C_2H_4)) = 8.42 \pm 0.05$ eV. Our calculations predict that the C_2H_4 binds to one Au atom, forming a T-shaped complex. The photoionization onset is due to removing an electron from the HOMO, which is primarily a *5s* orbital on the Au atom further from the C_2H_4. The increased photoionization yield above 9.5 eV is due to removing an electron from *4d* orbital(s) on one or both Au. The ionization energy of Au_2 is calculated to be 9.09 eV, in good agreement with the measured value of 9.20±0.21 eV.[55] This is slightly lower than IE(Au), but the bond dissociation energy of ethene to Au_2 is calculated to be 1.06 eV, significantly larger than in $Au(C_2H_4)$, while the bond dissociation energy of ethene to Au_2^+ is 1.99 eV, significantly smaller than in $Au^+(C_2H_4)$. There are only small changes in the geometry of $Au_2(C_2H_4)$ upon ionization, as shown in Figure 3, leading to a fairly sharp photoionization onset. More broadly, the calculations predict that the Au-Au bond lengths of Au_2 and Au_2^+ increase only 0.005 Å upon binding to C_2H_4. The C-C bonds in the neutral and cation lengthen considerably more, by about 0.05 Å. This is only slightly smaller than the lengthening observed upon Au^+ binding. Lang et al. measured the vibrational spectra of $Au_2^+(C_2H_4)$ and larger clusters in the fingerprint region using

IRMPD and a free-electron laser.[56] The vibrational spectrum is consistent with the π-bonded structure shown in Figure 3. Their calculations agree with ours, and both predict that binding to Au_2^+ induces substantial weakening of the C-C bond in ethylene, as do calculations on neutral $Au_2(C_2H_4)$ by Kang et al.[57]

C. Odd-Hydrogen Complexes

Although other structures are plausible, and in some cases are predicted to be more stable, the odd-hydrogen products have an AuH moiety. Reaction of laser-ablated gold atoms with ethylene produces AuH, as shown in Figure 1. Reaction with methane and acetylene also forms AuH, but to a lesser extent. A small amount of the very large Au^+ signal bleeds into the adjacent AuH^+ mass. This contribution has been removed in the PIE, shown in Figure 5. The PIE consists of a sharp onset at 10.3 eV, giving IE(AuH)=10.25±0.05 eV. Our calculations predict that AuH has a $^1\Sigma^+$ ground state with r_e=1.5393 Å, and AuH^+ has a $^2\Sigma^+$ ground state, with a nearly identical bond length of 1.5387 Å, as shown in Figure 6. Thus, the photoionization onset should be sharp, as is observed. The calculated ionization energy is 10.12 eV, in good agreement with experiment.

Although AuH emissions were observed[58] in the flame spectrum of gold in 1901, it took over two decades for the carrier of the bands to be identified.[59] Since, there have been numerous experimental studies of AuH, including electronic,[60-64] vibrational,[65-66] and rotational[67] spectra, as well as photoelectron spectroscopy of the anion.[68] There have also been many computational studies of AuH, as it is a benchmark system for high-level calculations of relativistic effects.[26, 69-74] Our calculated bond length r_e=1.5393 Å is slightly longer than the experimental value, r_e=1.5237 Å.[65] The experimental dissociation energy, D_0=3.22±0.13 eV, is derived from extrapolation of vibrational levels of the *a*, *b*, *c* and *B* excited electronic states, which dissociate to Au* ($^2D_{3/2}$).[62-63, 75] This value is slightly higher than our calculated D_0=2.91 eV.

Much less is known about AuH^+. The bond strength has been measured to be 2.13±0.11 eV from the endothermic reaction of Au^+ with H_2 and D_2,[76] and there have been several calculations on the ion.[69, 71, 77-80] Our calculated D_0=2.03 eV agrees with the experimental value. The bond strength of AuH can be determined by combining the experimental bond strength of AuH^+ and the ionization energies of gold and AuH:

$$D_0(Au\text{-}H) = D_0(Au^+\text{-}H) + IE(AuH) - IE(Au)$$

This gives $D_0(Au\text{-}H) = 3.15 \pm 0.12$ eV, which confirms the value inferred from AuH spectroscopy. This is a very high bond strength for a metal hydride, and much of the bond strength is due to relativistic effects.[26, 70, 72-73] As a result of its high stability, AuH is produced by the reactions of Au^+ with linear alkanes from propane to n-hexane.[13]

There is signal observed at 224 amu, the mass of [Au,C2,H3], from reaction of gold with ethylene and acetylene. However, its PIE is very inconsistent from scan to scan and is observed at very low photon energies, so much of it is likely due to the isobaric AuAl, which is produced by the laser striking the aluminum ablation block. This is supported by the observation of small amounts of signal at 27 amu (Al), 251 amu ($AuAl_2$) and 421 amu (Au_2Al). Reaction of laser-ablated gold atoms with ethylene produces the odd-hydrogen species [Au,C2,H5], whose PIE (Fig. 7) shows a fairly sharp onset at 9.35 eV. There are two likely structures. The lowest energy isomer is predicted to be $HAu(C_2H_4)$, an adduct of AuH with ethylene (Fig. 6), with a calculated ionization energy of 9.21 eV. The AuC_2H_5 isomer is calculated to lie 0.13 eV higher in energy, and to have an ionization energy of only 8.80 eV (to $AuC_2H_5^+$). The observed ionization energy of 9.35 ± 0.05 eV clearly favors $HAu(C_2H_4)$.

Several larger odd-hydrogen species are also observed: [Au,C4,H3] from acetylene and [Au,C4,H5] and [Au,C4,H7] from ethylene. Their PIEs are shown in Figure 8 and calculated low-lying structures for the neutrals and their corresponding cations are in Figure 9. The only odd-hydrogen species clearly observed in the reaction of gold with acetylene is [Au,C4,H3]. The PIE spectrum of [Au,C4,H3] (Fig. 8A) has a fairly gentle onset near 9 eV. The lowest-energy [Au,C4,H3] isomer is Au–C≡C–C(H)=CH_2 (Table S1) but it is calculated to have an ionization energy of only 8.36 eV. The gold alkyl complex H–C≡C-Au(C_2H_2), in which the Au is coordinated to the C-C triple bond in acetylene is predicted to be 0.37 eV higher in energy and to have an ionization energy of 8.93 eV. The calculations predict only a small geometry change on ionization, leading to a much sharper onset in the simulation than is observed experimentally. The $HAu(C_4H_2)$ isomer, in which the gold straddles a triple bond in diacetylene, is calculated to lie another 0.25 eV higher in energy. The calculated IE is 9.02 eV, also consistent with the experiment. Simulating the spectrum, including Franck-Condon factors, gives the PIE shown in Fig. 8A, which provides a good match to experiment. The calculations predict that there is a fairly large geometry change upon ionization, particularly in the H-Au-C angle and H-Au-C-H

torsion. This results in a gradual onset to the PIE curve, and an observed threshold ~0.2 eV above the adiabatic IE. The best fit to the experiment is IE=8.8 ± 0.1 eV, with the uncertainty reflecting the potential error in the calculated geometries. One concern is that we may be observing $HAu(C_4H_2)$ due to HAu clustering to a diacetylene impurity in the acetylene. The mass spectrum does have signal from C_4H_2, and the PIE matches that of diacetylene.[81] However, its intensity is only about a factor of four larger than that of [Au,C4,H3] and the calculated photoionization cross sections are similar, so its concentration is extremely low.

The PIE of [Au,C4,H5] is similar to that of [Au,C4,H3], with a fairly gentle onset near 9.1 eV (Figure 8B). This suggests that it has a similar structure, with an HAu core. The lowest energy [Au,C4,H5] isomer is calculated to be Au–C(H)=C(H)–C(H)=CH_2, in which gold replaces one of the terminal hydrogens in butadiene (Table S1). However, this isomer has a calculated ionization energy of only 8.24 eV and is not observed. A second isomer, HC≡C–$Au(C_2H_4)$ in which the gold alkyl AuCCH is coordinated to ethylene (Fig. 9) is calculated to lie only 0.13 eV higher in energy and to have an ionization energy of 8.98 eV. However, there is little geometry change on ionization, so the simulated PIE has a much sharper onset than is observed (Fig. 8B). A further 0.32 eV higher in energy is $HAu(C_4H_4)$, a complex of AuH with 1-buten-3-yne, with the Au coordinated to the triple bond (Fig. 9), which has a calculated ionization energy of 8.77 eV. As with $HAu(C_4H_2)$, there is substantial geometry change on ionization, especially in the H-Au-C angle and H-Au-C-H torsion. This again leads to a gradual onset of the PIE curve, with an observed threshold ~0.3 eV above the adiabatic IE, as shown by the simulation in Fig. 8B. A good fit to experiment is obtained with IE=8.8 ± 0.1 eV. The isomer with gold attached to the double bond is calculated to be 0.07 eV higher in energy and to have a similar IE. Two additional isomers are calculated to lie significantly higher in energy and to have low ionization energies: a $HAuC_4H_4$ metallocyclopentadiene and $HAu(C_2H_2)_2$, which are predicted to lie 1.10 and 1.63 eV above $HAu(C_4H_4)$, respectively and have IE's below 8.3 eV. They are likely not observed.

The PIE of [Au,C4,H7] (Fig. 8C) is qualitatively different from that of [Au,C4,H5]. Its onset occurs at much lower energy (~8.5 eV) and is more gradual. This suggests that the cation is substantially more strongly bound than the neutral and there is significant geometry change upon ionization. There are many possible isomers, and multiple isomers could contribute to the PIE. One low-energy structure is $HAu(C_4H_6)$ (Fig. S1), with the gold coordinated to a double bond in

butadiene. Its ionization energy is calculated to be 8.63 eV. As with $HAu(C_4H_4)$, there is substantial geometry change on ionization. The resulting shift in the ionization onset would likely place it above the experimental onset. A more likely contributor to the signal at low photon energy is $H_2C=C(H)–Au(C_2H_4)$, in which the gold is coordinated to the double bond in ethylene (Fig. S1). It is calculated to lie 0.31 eV above $HAu(C_4H_6)$ and to have an ionization energy of 8.17 eV. There is a large geometry change on ionization, and the vertical IE is calculated to be 8.90 eV. This could lead to the observed slow onset, and shift it to higher energy. In addition, there are several possible isomers that correspond to butene with gold replacing one hydrogen which lie at similar energies and have similar ionization energies. One representative gold-alkyl structure, $Au\text{-}CH_2CH_2CH=CH_2$, is shown in Fig. S1. It is 0.37 eV above $HAu(C_4H_6)$. It has IE=8.16 eV and a vertical IE of 8.97 eV, so the PIE would be very similar to that of $H_2C=C(H)–Au(C_2H_4)$. Two other structures are at substantially higher energy and have lower IEs and large geometry change on ionization. Although metallocycles are formed by intracluster reactions in $Ni^+(C_2H_2)_n$[82] and in sequential reactions of La atoms with acetylene and ethylene,[83-84] analogous gold-containing metallocycles are calculated to be energetically unfavorable. The metallocycle $HAu\text{-}C_4H_6$ in which the gold and carbons form a five-membered ring is 1.50 eV above $HAu(C_4H_6)$, and has an IE of only 7.31 eV. Even less likely is $HAu(C_2H_4)(C_2H_2)$, which has one ligand in the second shell, so it is quite weakly bound. It is 1.70 eV above $HAu(C_4H_6)$, and has an IE of 8.14 eV. Although the PIE is not definitive, the most likely structure is the $H_2C=C(H)–Au(C_2H_4)$ gold alkyl.

The observation of odd-hydrogen species is surprising. At room temperature and low pressures, no reaction is observed between gold atoms and ethylene,[14] as

$$Au + C_2H_4 \rightarrow AuH + C_2H_3$$

is endothermic by 1.5 eV. Production of AuH from acetylene is even more endothermic, by 2.6 eV. In our experiment, this reaction likely occurs due to production of translationally hot or electronically excited gold atoms in the ablation source. The lowest excited states of Au are $^2D_{5/2}$ at 1.136 eV and $^2D_{3/2}$ at 2.658 eV. Transitions from these states, which have a $\ldots 5d^9 6s^2$ electronic configuration, to the $^2S_{1/2}$ ($\ldots 5d^{10} 6s^1$) ground state are optically forbidden, so they are long lived. Subsequent clustering of gold hydride with acetylene or ethylene, respectively would produce $HAu(C_2H_2)$ and $HAu(C_2H_4)$. The calculations predict that these molecules are coordinatively saturated. Additional ligands form a second solvent shell, with very low bond

dissociation energies, so larger adducts are not observed. The gold alkyl $H_2C=C(H)–Au(C_2H_4)$ is likely produced by reaction of hot Au atoms:

$$Au + C_2H_4 \rightarrow AuC_2H_3 + H$$

followed by clustering with C_2H_4.

Our calculations show that AuH is intermediate between neutral gold atoms and Au^+ in its bond dissociation energies to ethylene and acetylene and the extent to which it distorts the geometry of the ligand, suggesting that it has potential for activation of unsaturated hydrocarbons. Although gold hydrides have long been proposed as reaction intermediates in homogeneous catalysis,[2] it took until 2008 for the first gold hydride to be isolated under preparative conditions. It was AuH complexed to the N-Heterocycle Carbene (NHC) 1,3-bis(2,6-diisopropylphenyl)imidazol-2-ylidene.[85] Gold hydride – NHC complexes are promising catalysts for olefin polymerization,[16] and investigations of their heterogeneous chemistry should advance rapidly with the availability of stabilized gold hydrides. It is thus possible that gas-phase AuH, which is coordinatively unsaturated, can sequentially react with C_2H_2 and C_2H_4 via C-C coupling and dehydrogenation to produce $HAu(C_4H_2)$ and $HAu(C_4H_4)$, respectively.

4. Summary and Conclusions

Laser-ablated gold atoms exhibit a surprisingly rich chemistry with acetylene and ethylene. The species produced are identified from their masses and by comparing their PIE curves to those calculated for potential isomers. This also determines their ionization energies. In addition to adducts such as $Au(C_2H_2)$ and $Au(C_2H_4)$, an adduct with gold dimer, $Au_2(C_2H_4)$, is observed. The most interesting species formed are a series of odd-hydrogen molecules that are identified to be gold hydrides, AuH, $HAu(C_2H_4)$ and $HAu(C_4H_x)$ (x=2, 4) which are likely produced by reaction of translationally or electronically excited gold atoms.

Acknowledgements

RBM gratefully acknowledges financial support from the National Science Foundation under Award No. CHE-1566407. We thank Professor Robert Lucchese for providing the *ePolyScat* software to calculate photoionization cross sections. This research used resources of the Advanced Light Source, which is a DOE Office of Science User Facility under contract no. DE-AC02-05CH11231. O.K. and M.A. were supported by the Director, Office of Science,

Office of Basic Energy Sciences, of the U.S. Department of Energy under the same contract, through the Gas Phase Chemical Physics Program of the Chemical Sciences Division.

Supporting Information

The Supporting Information is available free of charge on the ACS Publications Website at DOI: <Need to fill in>

Detailed procedure for calculating the photoionization cross sections.

Figure S1: PIE curve for $Au(C_2H_2)_2$, Figure S2: PIE curve and simulations for $Au^+(C_2H_4)$ and PIE curve for $Au^+(C_2H_4)_2$.

Table S1: Detailed structures and energies of gold-containing compounds calculated at the CAM-B3LYP/aug-cc-pVTZ level of theory.

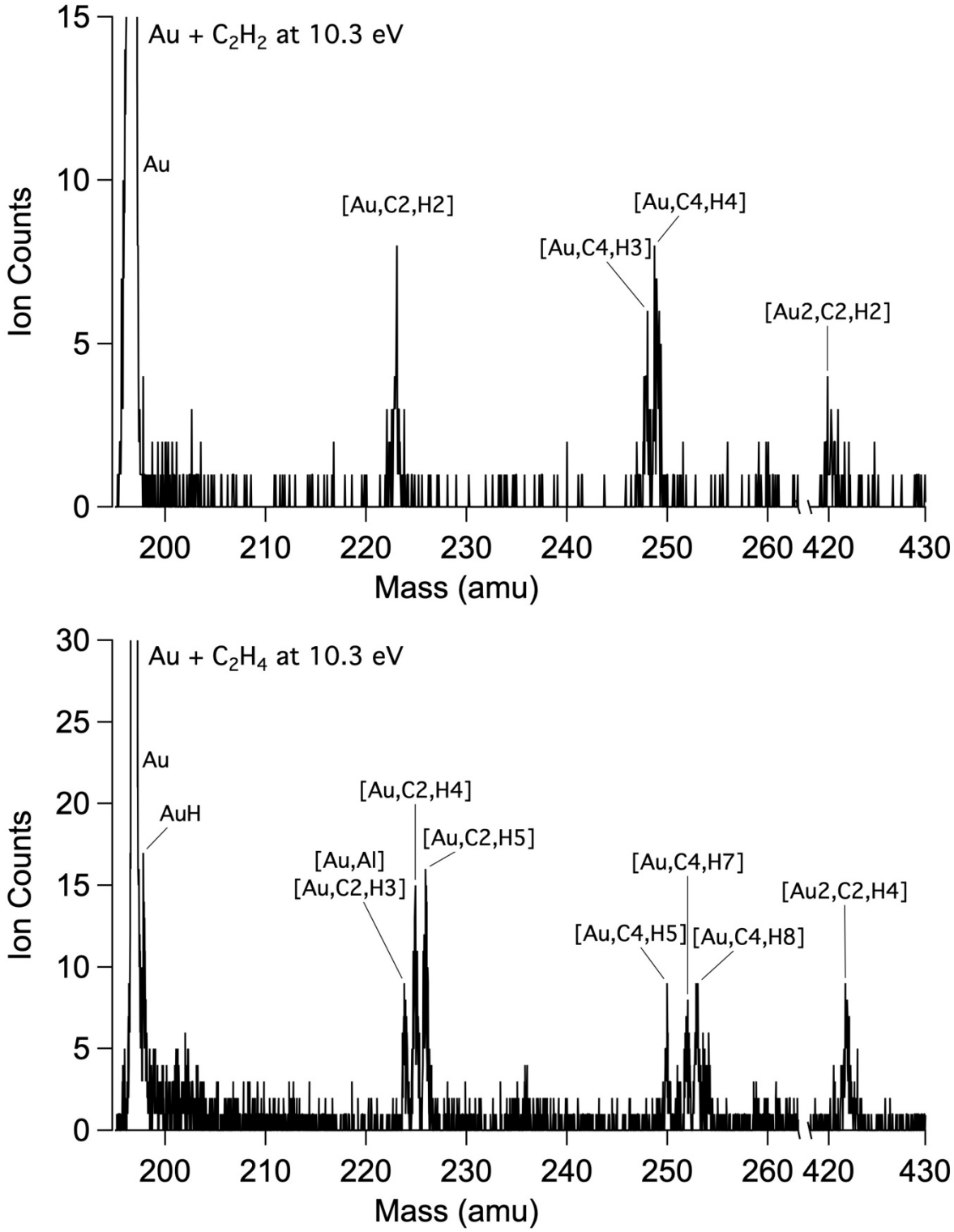

Figure 1: Mass spectra of reaction products of laser-ablated Au with C_2H_2 (top) and C_2H_4 (bottom) following VUV ionization at 10.3 eV. The Au signal is a factor of 10 larger than that of gold-containing molecules.

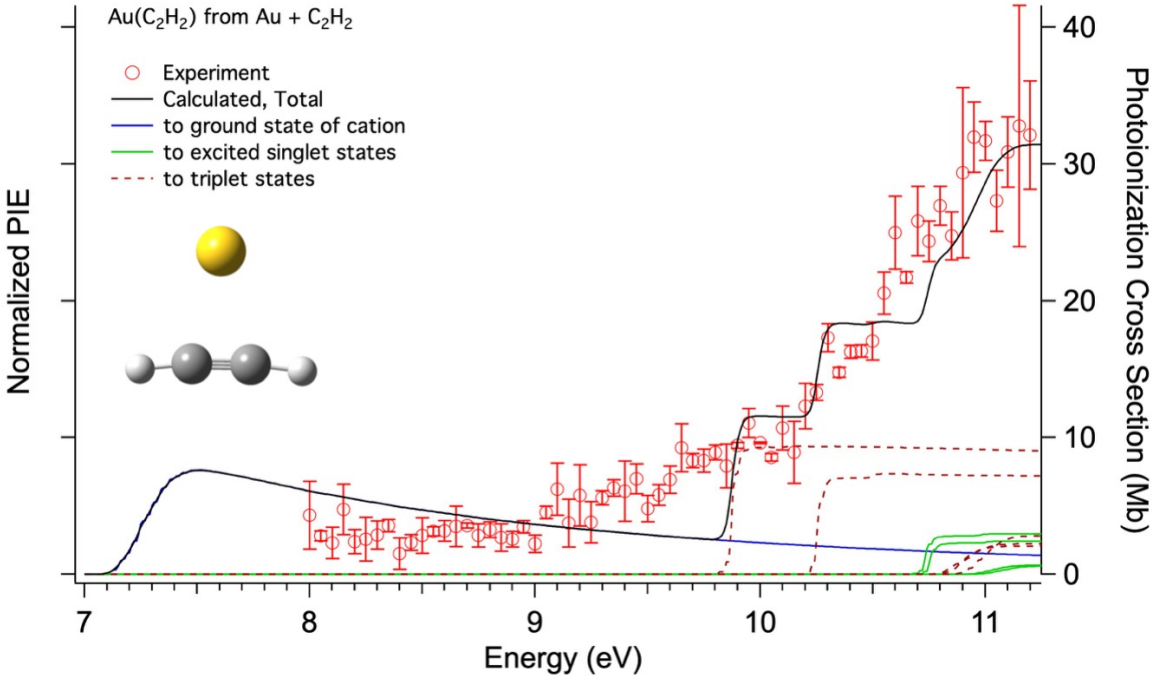

Figure 2: Measured and calculated PIE curve of $Au^{+}(C_2H_2)$.

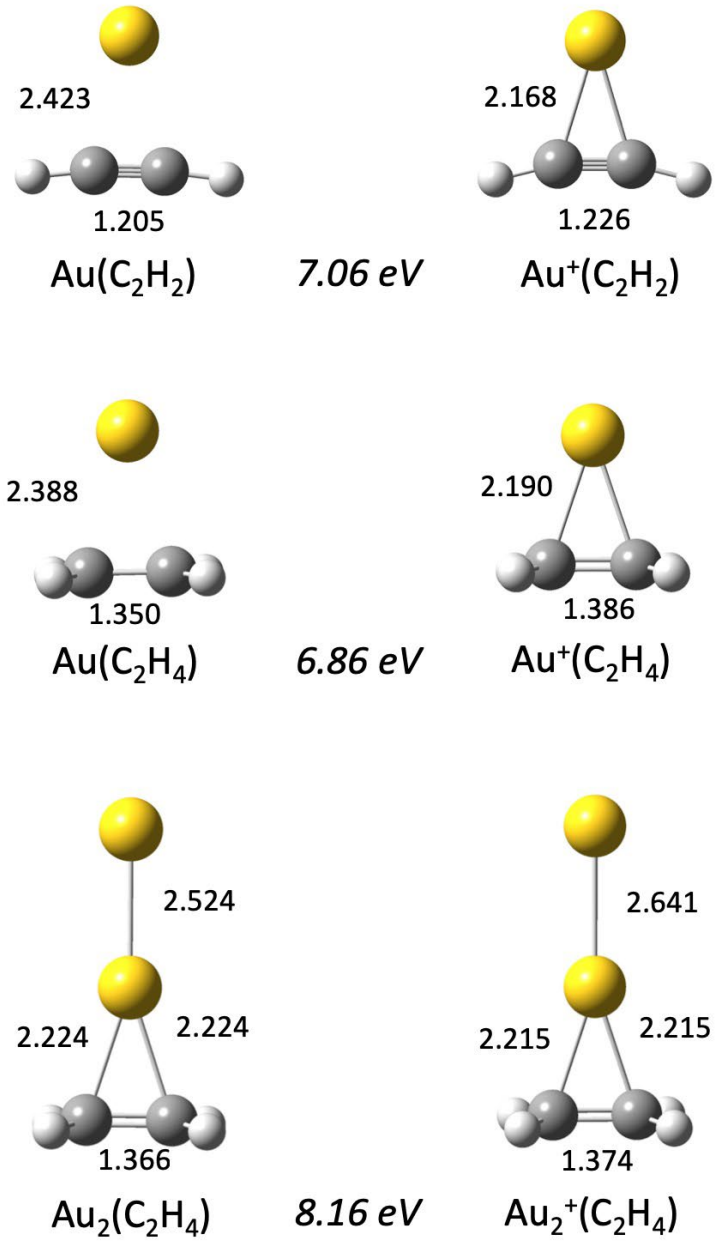

Figure 3: Structures of gold complexes with even numbers of hydrogens calculated at the CAM-B3LYP-aug-cc-pVTZ level. Key bond lengths are in Å. Ionization energies are in italics.

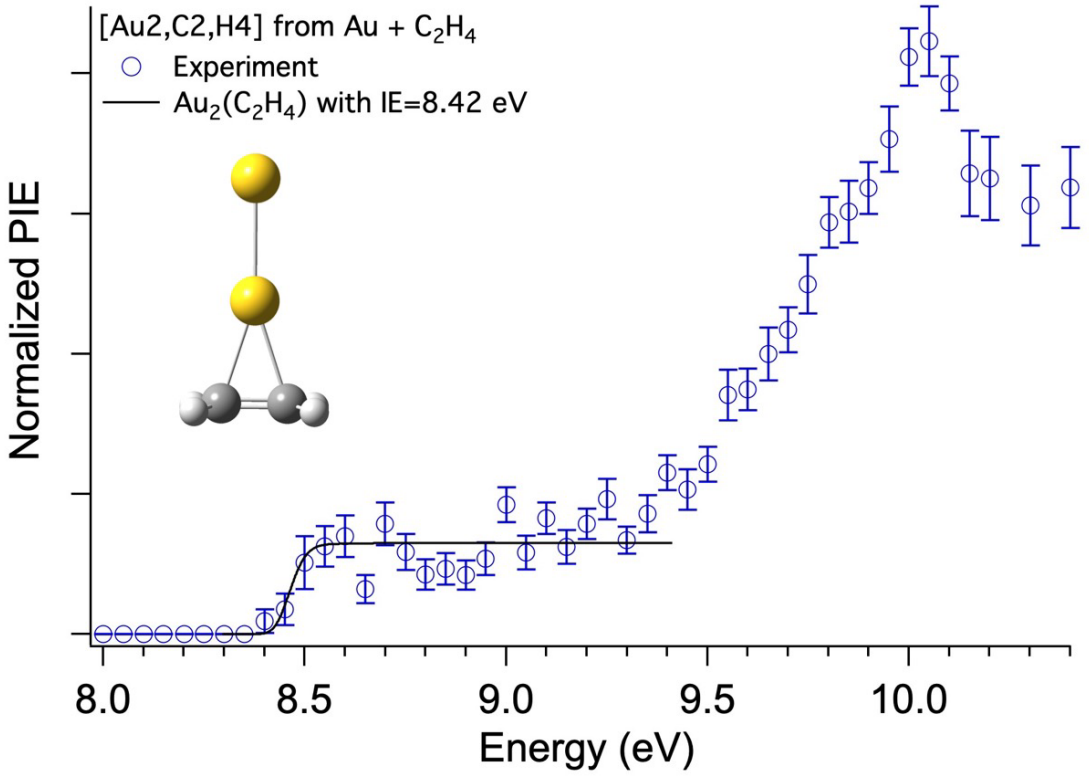

Figure 4: Measured and simulated PIE curve of $Au_2(C_2H_4)$.

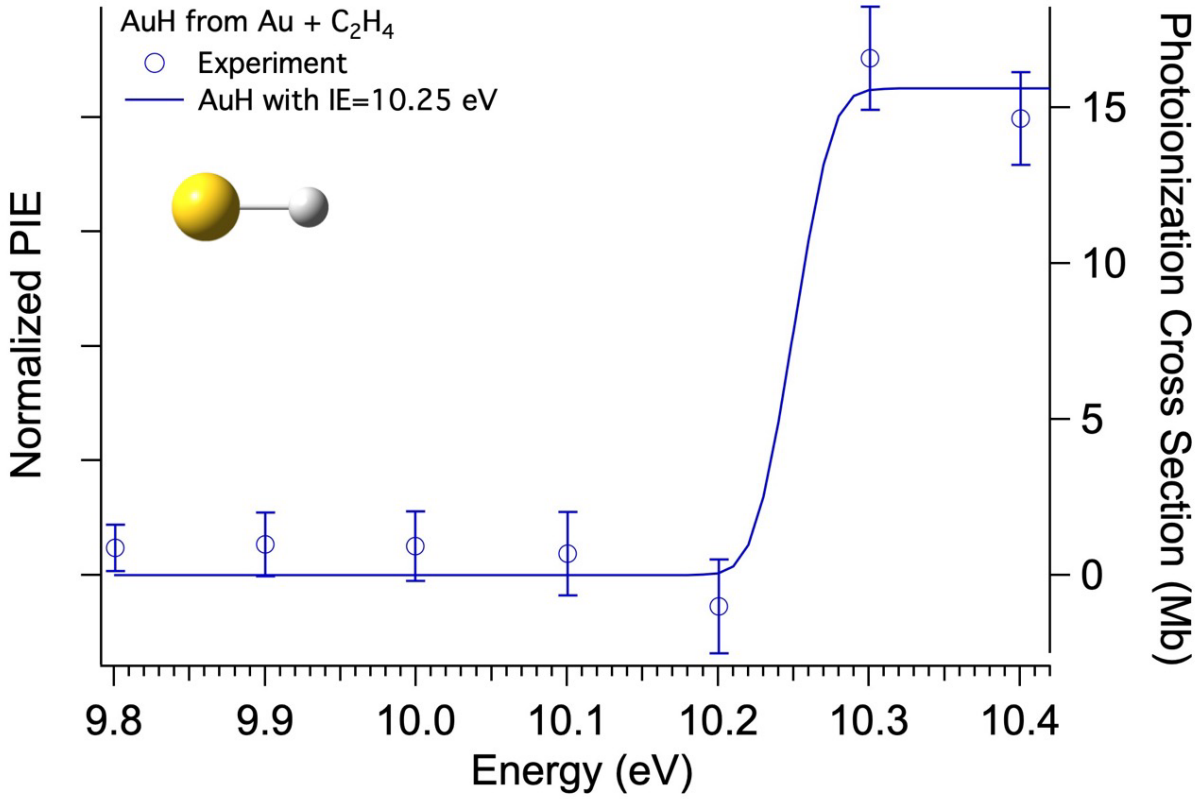

Figure 5: Measured and simulated PIE curve of AuH.

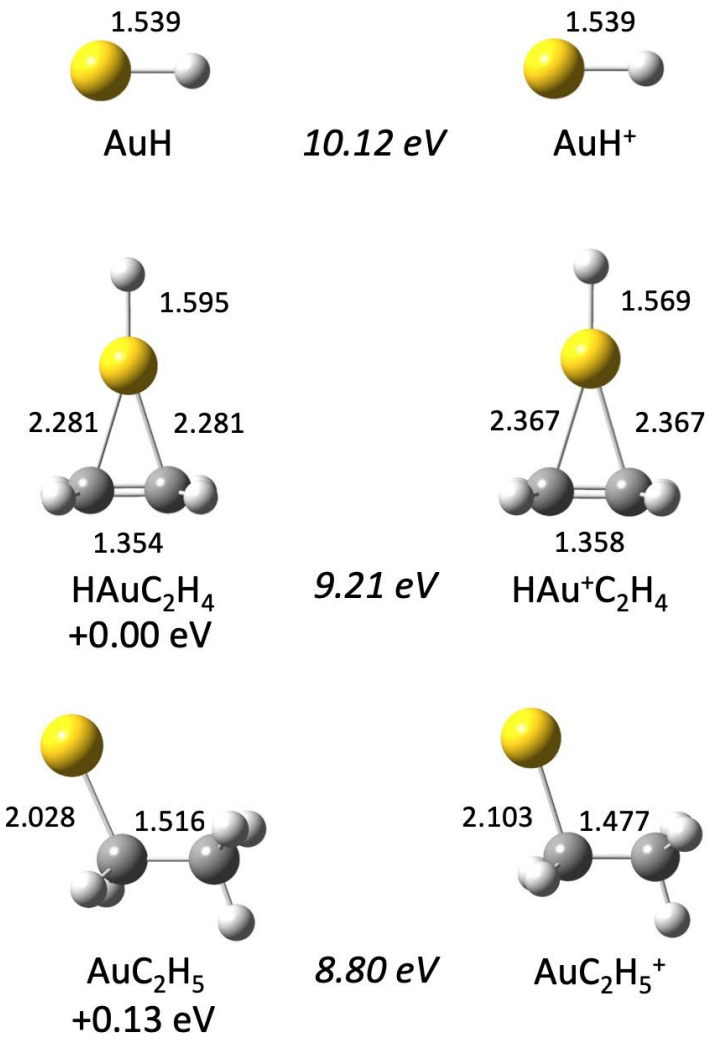

Figure 6: Structures of smaller gold complexes with odd numbers of hydrogens calculated at the CAM-B3LYP-aug-cc-pVTZ level. Bond lengths are in Å. Ionization energies are in italics. Relative energies of neutral isomers are given below the structures.

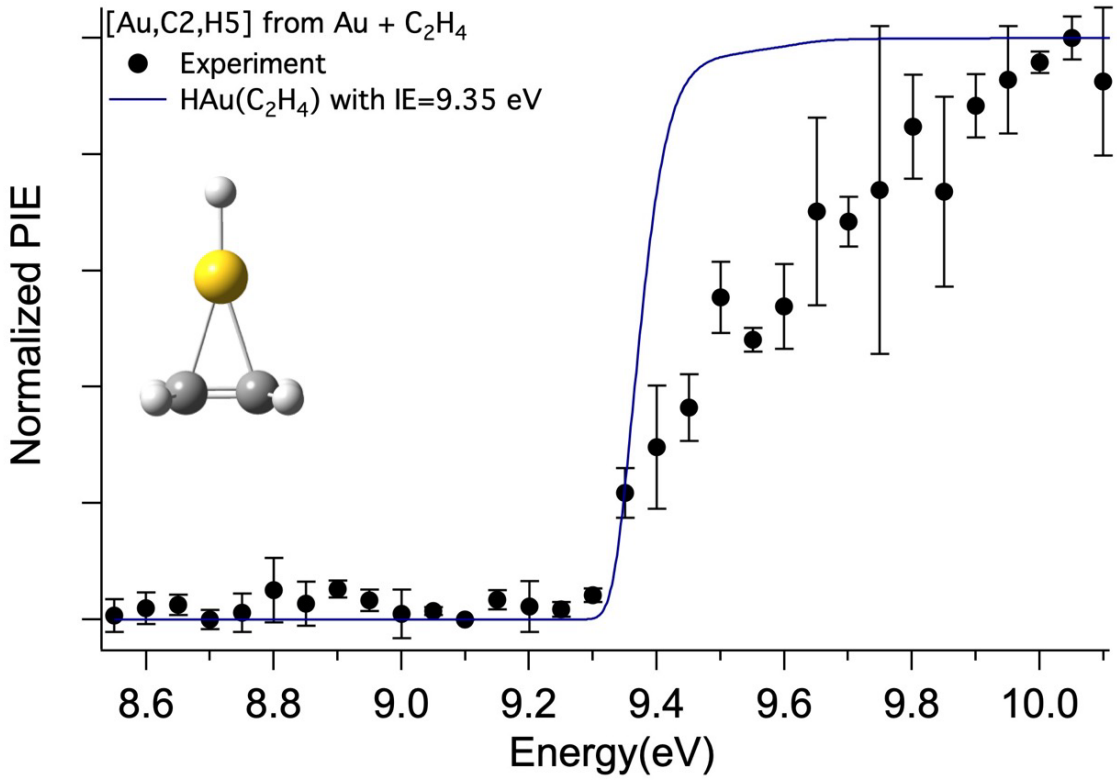

Figure 7: Measured and simulated PIE curve of $HAu(C_2H_4)$.

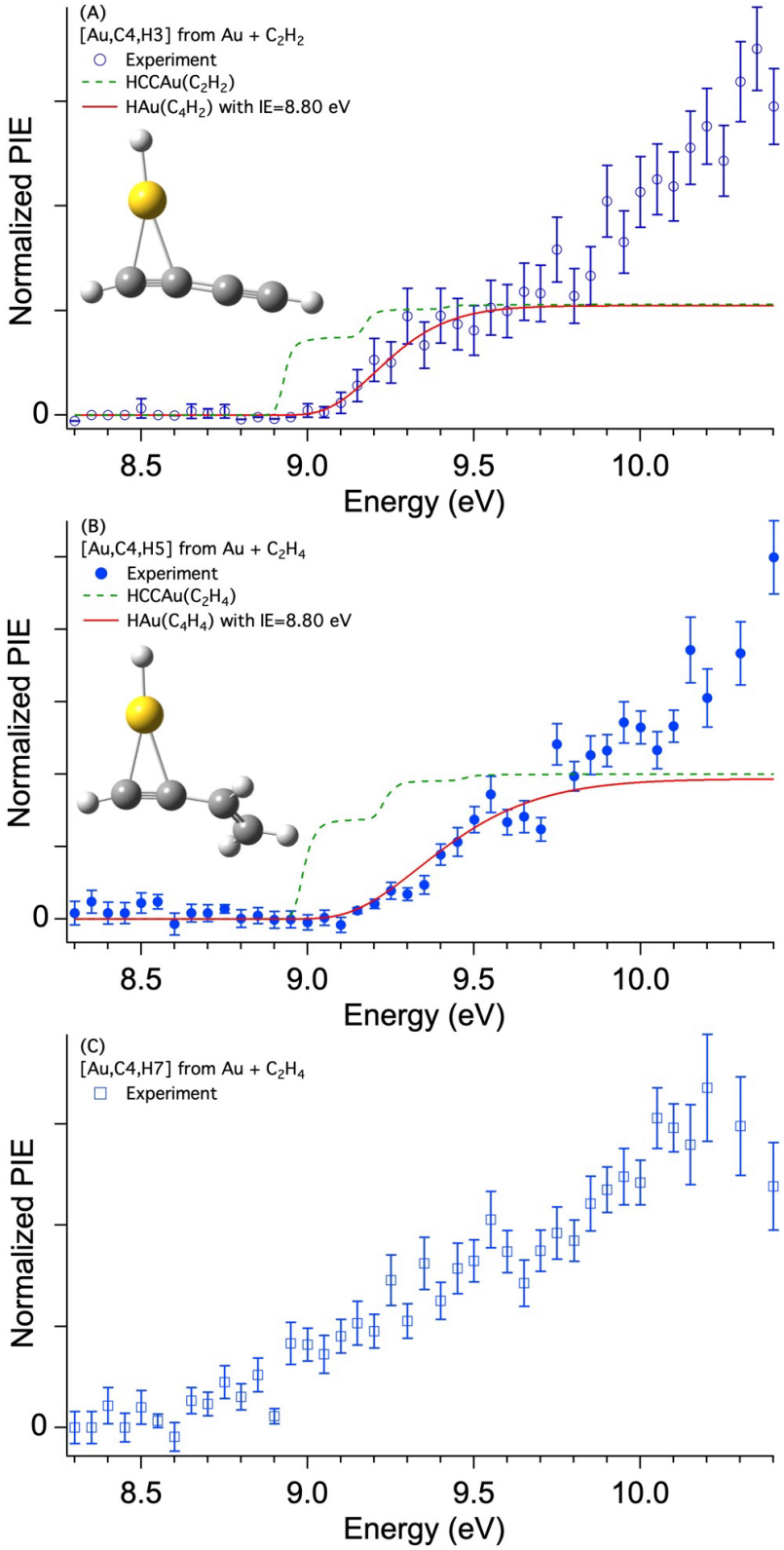

Figure 8: Experimental and simulated PIEs of A) [Au,C4,H3], B) [Au,C4,H5] and C) [Au,C4,H7].

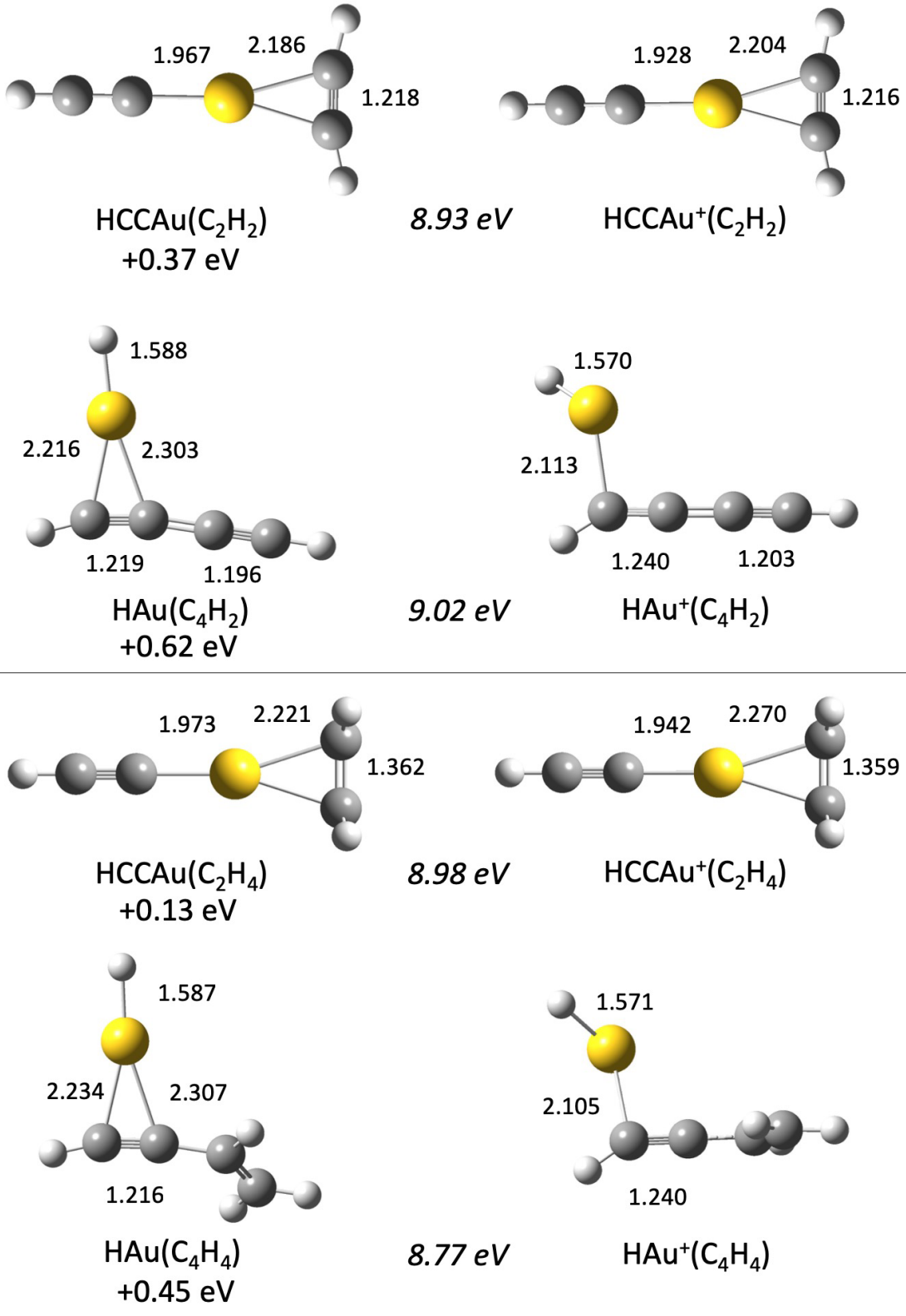

Figure 9: Structures of [Au,C4,H3] and [Au,C4,H5] neutrals and cations calculated at the CAM-B3LYP-aug-cc-pVTZ level, with bond lengths in Å. Ionization energies are in italics. Energies of neutral isomers, relative to the lowest-energy isomer, are given below the structures.

Species	Calculated	Experiment
Au	9.24	9.226 [37]
$Au(C_2H_2)$	7.06	< 8.0
$Au(C_2H_4)$	6.86	< 8.0
AuH	10.12	10.25±0.05
$HAu(C_2H_2)$	9.31	
$HAu(C_2H_4)$	9.21	9.35±0.05
AuC_2H_5	8.80	
$HAu(C_4H_2)$	9.02	8.8±0.1
$HAu(C_4H_4)$	8.77	8.8±0.1
$HAu(C_4H_6)$	8.63	
$H_2C=C(H)-Au(C_2H_4)$	8.17	
$Au-CH_2CH_2CH=CH_2$	8.16	
Au_2	9.09	9.20±0.21 [55]
$Au_2(C_2H_4)$	8.16	8.42±0.05

Table 1: Measured and calculated (CAM-B3LYP/aug-cc-pVTZ) adiabatic ionization energies, in eV. Measured values are from this work, unless otherwise noted.

Species	Neutral	Cation
$Au–C_2H_2$	0.16	2.35
$Au–C_2H_4$	0.24	2.62
Au–H	2.91	2.03
$HAu–C_2H_2$	0.90	1.72
$HAu–C_2H_4$	0.95	1.86
$HAu–C_4H_2$	0.80	1.91
$HAu–C_4H_4$	0.91	2.26
$HAu–C_4H_6$	0.91	2.40
Au–Au	1.92	2.07
$Au_2–C_2H_4$	1.06	1.99

Table 2: Calculated (CAM-B3LYP/aug-cc-pVTZ) bond dissociation energies, in eV.

References

1. Bond, G. C.; Louis, C.; Thompson, D. T., *Catalysis by Gold*. Imperial College Press: London, 2006.
2. Hashmi, A. S. K.; Hutchings, G. J. Gold Catalysis. *Angew. Chem. Int. Ed.* **2006,** *45*, 7896 – 7936.
3. Gorin, D. J.; Toste, F. D. Relativistic Effects in Homogeneous Gold Catalysis. *Nature* **2007,** *446*, 395-403.
4. Dias, H. V. R.; Wu, J. Structurally Characterized Coinage-Metal–Ethylene Complexes. *Eur. J. Inorg. Chem.* **2008**, 509-522.
5. Li, Z.; Brouwer, C.; He, C. Gold-Catalyzed Organic Transformations. *Chem. Rev.* **2008,** *108*, 3239–3265.
6. Pflästerer, D.; Hashmi, A. S. K. Gold Catalysis in Total Synthesis – Recent Achievements. *Chem. Soc. Rev.* **2016,** *45*, 1331-1367.
7. Teles, J. H.; Brode, S.; Chabanas, M. Cationic Gold(i) Complexes: Highly Efficient Catalysts for the Addition of Alcohols to Alkynes. *Ang. Chem. Int. Ed.* **1998,** *37*, 1415-1418.
8. Schmidbaur, H.; Schier, A. Gold η^2-Coordination to Unsaturated and Aromatic Hydrocarbons: The Key Step in Gold-Catalyzed Organic Transformations. *Organometallics* **2010,** *29*, 2-23.
9. Kang, R.; Chen, H.; Shaik, S.; Yao, J. Assessment of Theoretical Methods for Complexes of Gold(I) and Gold(III) with Unsaturated Aliphatic Hydrocarbon: Which Density Functional Should We Choose? *J. Chem. Theory Comput.* **2011,** *7*, 4002–4011.
10. Schröder, D.; Hrusák, J.; Hertwig, R. H.; Koch, W.; Schwerdtfeger, P.; Schwarz, H. Experimental and Theoretical Studies of Gold(I) Complexes $Au(L)^+$ (L = H_2O, CO, NH_3, C_2H_4, C_3H_6, C_4H_6, C_6H_6, C_6F_6). *Organometallics* **1995,** *14*, 312-316.
11. Roithová, J.; Schröder, D. Theory Meets Experiment: Gas-Phase Chemistry of Coinage Metals. *Coord. Chem. Rev.* **2009,** *253*, 666–677.
12. Roithova, J.; Schröder, D. Selective Activation of Alkanes by Gas-Phase Metal Ions. *Chem. Rev.* **2010,** *110*, 1170-1211.
13. Zhang, T.; Li, Z.-Y.; Zhang, M.-Q.; He, S.-G. Gas-Phase Reactions of Atomic Gold Cations with Linear Alkanes (C2−C9). *J. Phys. Chem. A* **2016,** *120*, 4285-4293.
14. Carroll, J. J.; Weisshaar, J. C. Gas Phase Kinetics of Neutral Transition Metal Atoms: Reactions of Hf, Ta, Ir, Pt, and Au with Alkanes and Alkenes. *J. Phys. Chem.* **1996,** *100*, 12355-12363.
15. Ito, H.; Saito, T.; Miyahara, T.; Zhong, C. M.; Sawamura, M. Gold(I) Hydride Intermediate in Catalysis: Dehydrogenative Alcohol Silylation Catalyzed by Gold(I) Complex. *Organometallics* **2009,** *28*, 4829-4840.
16. Klatt, G.; Xu, R.; Pernpointner, M.; Molinari, L.; Hung, T. Q.; Rominger, F.; Hashmi, A. S. K.; Köppel, H. Are β-H-Eliminations or Alkene Insertions Feasible Elementary Steps in Catalytic Cycles Involving Gold(I) Alkyl Species or Gold(I) Hydrides? *Chem. Eur. J.* **2013,** *19*, 3954-3961.
17. Nicolas, C.; Shu, J.; Peterka, D. S.; Poisson, L.; Leone, S. R.; Ahmed, M. Vacuum Ultraviolet Photoionization of C_3. *J. Am. Chem. Soc.* **2006,** *128*, 220-226.
18. Leone, S. R.; Ahmed, M.; Wilson, K. R. Chemical Dynamics, Molecular Energetics, and Kinetics at the Synchrotron. *Phys. Chem. Chem. Phys.* **2010,** *12*, 6564-6578.

19. Golan, A.; Ahmed, M. Molecular beam mass spectrometry with tunable vacuum ultraviolet (VUV) synchrotron radiation. *J. Vis. Exp.* **2012,** *68*, e50164.
20. Kostko, O.; Bandyopadhyay, B.; Ahmed, M. Vacuum Ultraviolet Photoionization of Complex Chemical Systems. *Ann. Rev. Phys. Chem.* **2016,** *67*, 19-40.
21. Metz, R. B.; Nicolas, C.; Ahmed, M.; Leone, S. R. Direct Determination of the Ionization Energies of FeO and CuO with VUV Radiation. *J. Chem. Phys.* **2005,** *123*, 114313-6.
22. Citir, M.; Metz, R. B.; Belau, L.; Ahmed, M. Direct Determination of the Ionization Energies of PtO, PtO_2 and PtC with VUV Radiation. *J. Phys. Chem. A* **2008,** *112*, 9584-9590.
23. Perera, M.; Metz, R. B.; Kostko, O.; Ahmed, M. Vacuum Ultraviolet Photoionization Studies of $PtCH_2$ and H-Pt-CH_3: A Potential Energy Surface for the Pt + CH_4 Reaction. *Angew. Chem. Int. Ed.* **2013,** *52*, 888-891.
24. Perera, M.; Roenitz, K. M.; Metz, R. B.; Kostko, O.; Ahmed, M. VUV Photoionization Measurements and Electronic Structure Calculations of the Ionization Energies of Gas-Phase Tantalum Oxides: TaO_x (x=3-6). *J. Spectrosc. Dyn.* **2014,** *4*, 21-10.
25. Schwarz, H. Relativistic Effects in Gas-Phase Ion Chemistry: An Experimentalist's View. *Angew. Chem. Int. Ed.* **2003,** *42*, 4442-4454.
26. Pyykkö, P. Theoretical Chemistry of Gold. *Angew. Chem.-Int. Ed.* **2004,** *43*, 4412-4456.
27. Pyykkö, P. Theoretical Chemistry of Gold. II. *Inorg. Chim. Acta* **2005,** *358*, 4113-4130.
28. Pyykkö, P. Theoretical Chemistry of Gold. III. *Chem. Soc. Rev.* **2008,** *37*, 1967-1997.
29. Frisch, M. J.; Trucks, G. W.; Schlegel, H. B.; Scuseria, G. E.; Robb, M. A.; Cheeseman, J. R.; Scalmani, G.; Barone, V.; Mennucci, B.; Petersson, G. A., et al. *Gaussian 09, Rev. D.01*, Gaussian, Inc., Wallingford, CT, Pittsburgh PA, 2010.
30. Figgen, D.; Peterson, K. A.; Dolg, M.; Stoll, H. Energy-consistent Pseudopotentials and Correlation Consistent Basis Sets for the 5d elements Hf–Pt. *J. Chem. Phys.* **2009,** *130*, 164108-12.
31. Fang, H.-C.; Li, Z. H.; Fan, K.-N. CO Oxidation Catalyzed by a Single Gold Atom: Benchmark Calculations and the Performance of DFT Methods. *Phys. Chem. Chem. Phys.* **2011,** *13*, 13358-13369.
32. Taatjes, C. A.; Osborn, D. L.; Cool, T. A.; Nakajima, K. Synchrotron Photoionization Measurements of Combustion Intermediates: The Photolonization Efficiency of HONO. *Chem. Phys. Lett.* **2004,** *394*, 19-24.
33. Lucchese, R. R.; Sanna, N.; Natalense, A. P. P.; Gianturco, F. A.
ePolyScat, version E3.
34. Gianturco, F. A.; Lucchese, R. R.; Sanna, N. Calculation of Low-Energy Elastic Cross Sections for Electron-CF_4 Scattering. *J. Chem. Phys.* **1994,** *100*, 6464-6471.
35. Natalense, A. P. P.; Lucchese, R. R. Cross Section and Asymmetry Parameter Calculation for Sulfur 1s Photoionization of SF_6. *J. Chem. Phys.* **1999,** *111*, 5344-5348.
36. Gans, B.; Boye-Peronne, S.; Broquier, M.; Delsaut, M.; Douin, S.; Fellows, C. E.; Halvick, P.; Loison, J.-C.; Lucchese, R. R.; Gauyacq, D. Photolysis of Methane Revisited at 121.6 nm and at 118.2 nm: Quantum Yields of the Primary Products, Measured by Mass Spectrometry. *Phys. Chem. Chem. Phys.* **2011,** *13*, 8140-8152.
37. Dyubko, S. F.; Efremov, V. A.; Gerasimov, V. G.; MacAdam, K. B. Millimetre-Wave Spectroscopy of Au I Rydberg States: S, P and D Terms. *J. Phys. B: At. Mol. Opt. Phys* **2005,** *38*, 1107-1118.
38. Kasai, P. H. Acetylene and Ethylene Complexes of Gold Atoms: Matrix Isolation ESR Study. *J. Am. Chem. Soc.* **1983,** *105*, 6704-6710.

39. Chenier, J. H. B.; Howard, J. A.; Mile, B.; Sutcliffe, R. Cryochemical Studies. 3. ESR Studies of the Reaction of Group 1B Metal Atoms with Acetylene and Phenylacetylene in a Rotating Cryostat. *J. Am. Chem. Soc.* **1983,** *105*, 788-791.
40. Zoellner, R. W.; Klabunde, K. J. Alkynes and Metal Atoms. *Chem. Rev.* **1984,** *84*, 545-559.
41. Roithová, J.; Hrusák, J.; Schröder, D.; Schwarz, H. A Gas-Phase Study of the Gold-Catalyzed Coupling of Alkynes and Alcohols. *Inorg. Chim. Acta* **2005,** *358*, 4287–4292.
42. Ward, T. B.; Brathwaite, A. D.; Duncan, M. A. Infrared Spectroscopy of Au(Acetylene)$_n^+$ Complexes in the Gas Phase. *Top. Catal.* **2018,** *61*, 49-61.
43. Dewar, M. J. S.; Ford, G. P. Relationship between Olefinic Π Complexes and Three-Membered Rings. *J. Am. Chem. Soc.* **1979,** *101*, 783-791.
44. Michael, D.; Mingos, P. J. A Historical Perspective on Dewar's Landmark Contribution to Organometallic Chemistry. *Organomet. Chem.* **2001,** *635*, 1-8.
45. McIntosh, D.; Ozin, G. A. Direct Synthesis Using Gold Atoms: Synthesis, Infrared and Ultraviolet-Visible Spectra and Molecular Orbital Investigations of Monoethylene Gold(0), (C_2H_4)Au. *J. Organomet. Chem.* **1976,** *121*, 127-136.
46. Hertwig, R. H.; Koch, W.; Schröder, D.; Schwarz, H.; Hrusák, J.; Schwerdtfeger, P. A Comparative Computational Study of Cationic Coinage Metal-Ethylene Complexes (C_2H_4)M^+ (M=Cu, Ag, and Au). *J. Phys. Chem.* **1996,** *100*, 12253-12260.
47. Nechaev, M. S.; Rayón, V. M.; Frenking, G. Energy Partitioning Analysis of the Bonding in Ethylene and Acetylene Complexes of Group 6, 8, and 11 Metals: $(CO)_5TM\text{-}C_2H_x$ and $Cl_4TM\text{-}C_2H_x$ (TM = Cr, Mo, W), $(CO)_4TM\text{-}C_2H_x$ (TM = Fe, Ru, Os), and $TM^+\text{-}C_2H_x$ (TM = Cu, Ag, Au). *J. Phys. Chem. A* **2004,** *108*, 3134-3142.
48. Li, J.; Zhou, S.; Schlangen, M.; Weiske, T.; Schwarz, H. Hidden Hydride Transfer as a Decisive Mechanistic Step in the Reactions of the Unligated Gold Carbide $[AuC]^+$ with Methane under Ambient Conditions. *Ang. Chem. Int. Ed.* **2016,** *55*, 13072-13075.
49. Buratto, S. K.; Bowers, M. T.; Metiu, H.; Manard, M.; Tong, X.; Benz, L.; Kemper, P.; Chrétien, S., Au_n and Ag_n (n =1–8) Nanocluster Catalysts: Gas-phase Reactivity to Deposited Structures. In *Atomic Clusters: From Gas Phase to Deposited*, Woodruff, D. P., Ed. Elsevier: Amsterdam, 2007.
50. Schröder, D.; Schwarz, H.; Hrusák, J.; Pyykkö, P. Cationic Gold(I) Complexes of Xenon and of Ligands Containing the Donor Atoms Oxygen, Nitrogen, Phosphorus, and Sulfur. *Inorg. Chem.* **1998,** *37*, 624-632.
51. Stringer, K. L.; Citir, M.; Metz, R. B. Photofragment Spectroscopy of Pi Complexes: Au^+(C_2H_4) and Pt^+(C_2H_4). *J. Phys. Chem. A* **2004,** *108*, 6996-7002.
52. Metz, R. B. Spectroscopy of the Potential Energy Surfaces for C-H and C-O Bond Activation by Transition Metal and Metal Oxide Cations. *Adv. Chem. Phys.* **2008,** *138*, 331-373.
53. Mendizabal, F. Theoretical Study of the Au-Ethylene Interaction. *Int. J. Quantum Chem.* **1999,** *73*, 317.
54. Sodupe, M.; Bauschlicher Jr., C. W.; Langhoff, S. R.; Partridge, H. Theoretical Study of the Bonding of the First-Row Transition-Metal Positive Ions to Ethylene. *J. Phys. Chem.* **1992,** *96*, 2118-2122.
55. Bishea, G. A.; Morse, M. D. Spectroscopic Studies of Jet-Cooled AgAu and Au_2. *J. Chem. Phys.* **1991,** *95*, 5646-5659.
56. Lang, S. M.; Bernhardt, T. M.; Bakker, J. M.; Yoon, B.; Landman, U. The Interaction of Ethylene with Free Gold Cluster Cations: Infrared Photodissociation Spectroscopy Combined

with Electronic and Vibrational Structure Calculations. *J. Phys.: Condens. Matter* **2018,** *30*, 504001-11.
57. Kang, G.-J.; Chen, Z.-X.; Li, Z. Theoretical Studies of the Interactions of Ethylene and Formaldehyde with Gold Clusters. *J. Chem. Phys.* **2009,** *131*, 034710-8.
58. Hartley, W. N.; Ramage, H. Banded Flame-Spectra of Metals. *Trans. Roy. Dublin Soc.* **1901,** *7*, 339-352.
59. Bengtsson, E. Die Kombinationsbeziehungen bei den Bandenspektren der Goldflamme. *Ark. Mat. Astr. Fys.* **1925,** *18*, 1-9.
60. Hulthén, E.; Zumstein, R. V. The Absorption Spectra of Some Hydride Compounds in the Ultra-violet. *Phys. Rev.* **1926,** *28*, 13-24.
61. Farkas, A. Über die Bildung von Gasförmigem Goldhydrid. *Z. Phys. Chem. Abt. B* **1929,** *5*, 467-475.
62. Ringström, U. Absorption Spectrum of Gold Hydride in Ultra-violet. *Nature* **1963,** *198*, 981.
63. Ringström, U. Absorption Spectra of Gold Hydride and Gold Deuteride in Far Ultraviolet. *Ark. Fys.* **1964,** *27*, 227-265.
64. Fellows, C. E.; Rosberg, M.; Campos, A. P. C.; Gutteres, R. F.; Amiot, C. The AuH A $O^+ \rightarrow X\ ^1\Sigma^+$ System. *J. Mol. Spectrosc.* **1997,** *185*, 420-421.
65. Seto, J. Y.; Morbi, Z.; Charron, F.; Lee, S. K.; Bernath, P. F.; Le Roy, R. J. Vibration-Rotation Emission Spectra and Combined Isotopomer Analyses for the Coinage Metal Hydrides: CuH & CuD, AgH & AgD, and AuH & AuD. *J. Chem. Phys.* **1999,** *110*, 11756-11767.
66. Wang, X.; Andrews, L. Infrared Spectra and DFT Calculations for the Gold Hydrides AuH, $(H_2)AuH$, and the AuH_3 Transition State Stabilized in $(H_2)AuH_3$. *J. Phys. Chem. A* **2002,** *106*, 3744-3748.
67. Okabayashi, T.; Okabayashi, E. Y.; Tanimoto, M.; Furuya, T.; Saito, S. Rotational Spectroscopy of AuH and AuD in the $^1\Sigma^+$ Electronic Ground State. *Chem. Phys. Lett.* **2006,** *422*, 58–61.
68. Wu, X.; Qin, Z. B.; Xie, H.; Cong, R.; Wu, X. H.; Tang, Z. C.; Fan, H. J. Vibrationally Resolved Photoelectron Imaging of Gold Hydride Cluster Anions: AuH^- and Au_2H^-. *J. Chem. Phys.* **2010,** *133*, 044303.
69. Schwerdtfeger, P.; Dolg, M.; Schwarz, W. H. E.; Bowmaker, G. A.; Boyd, P. D. W. Relativistic Effects in Gold Chemistry. I. Diatomic Gold Compounds. *J. Chem. Phys.* **1989,** *91*, 1762-.
70. Kaldor, U.; Hess, B. A. Relativistic All-electron Coupled-cluster Calculations on the Gold Atom and Gold Hydride in the Framework of the Douglas-Kroll Transformation. *Chem. Phys. Lett.* **1994,** *230*, 1-7.
71. Kaldor, U.; Hess, B. A. Relativistic All-Electron Coupled-Cluster Calculations on the Gold Atom and Gold Hydride in the Framework of the Douglas-Kroll Transformation. *Chem. Phys. Lett.* **1994,** *230*, 1-7.
72. Lee, H.-S.; Han, Y.-K.; Kim, M. C.; Bae, C.; Lee, Y. S. Spin-orbit Effects Calculated by Two-Component Coupled-Cluster methods: Test calculations on AuH, Au_2, TlH and Tl_2. *Chem. Phys. Lett.* **1998,** *293*, 97-102.
73. Schwerdtfeger, P.; Brown, J. R.; Laerdahl, J. K.; Stoll, H. The Accuracy of the Pseudopotential Approximation. III. A Comparison between Pseudopotential and All-electron Methods for Au and AuH. *J. Chem. Phys.* **2000,** *113*, 7110-7118.

74. Yuan, M.; Li, W.; Yuan, J.; Chen, M. A Global Potential Energy Surface and Time-Dependent Quantum Wave Packet Calculation of Au + H_2 Reaction. *Int. J. Quantum Chem.* **2017,** *118*, e25493-10.
75. Huber, K. P.; Herzberg, G., *Molecular Spectra and Molecular Structure. IV. Constants of Diatomic Molecules*. Van Nostrand: New York, 1974.
76. Li, F.; Hinton, C. S.; Citir, M.; Liu, F.; Armentrout, P. B. Guided Ion Beam and Theoretical Study of the Reactions of Au^+ with H_2, D_2, and HD. *J. Chem. Phys.* **2011,** *134*, 024310-10.
77. Ohanessian, G.; Brusich, M. J.; Goddard III, W. A. Theoretical Study of Transition Metal Hydrides. 5. Hafnium to Mercury (HfH^+ through HgH^+), Barium and Lanthanum (BaH^+, and LaH^+). *J. Am. Chem. Soc.* **1990,** *112*, 7179-7189.
78. Ishikawa, Y.; Malli, G. L.; Pyper, N. C. Ab initio Dirac-Fock Self-Consistent Field Calculations for Open-Shell Heavy-Atom Systems: Bonding in AuH^+ Ion. *Chem. Phys. Lett.* **1992,** *194*, 481-484.
79. Hrusák, J.; Hertwig, R. H.; Schröder, D.; Schwerdtfeger, P.; Koch, W.; Schwarz, H. Relativistic Effects in Cationic Gold(I) Complexes - A Comparative Study of ab initio Pseudopotential and Density-Functional Methods. *Organometallics* **1995,** *14*, 1284-1291.
80. Dorta-Urra, A.; Zanchet, A.; Roncero, O.; Aguado, A.; Armentrout, P. B. Communication: Theoretical Exploration of $Au^+ + H_2$, D_2, and HD Reactive Collisions. *J. Chem. Phys.* **2011,** *135*, 091102-4.
81. Goulay, F.; Osborn, D. L.; Taatjes, C. A.; Zou, P.; Meloni, G.; Leone, S. R. Direct Detection of Polyynes Formation from the Reaction of Ethynyl Radical (C_2H) with Propyne (CH_3–C≡CH) and Allene (CH_2=C=CH_2). *Phys. Chem. Chem. Phys.* **2007,** *9*, 4291–4300.
82. Walters, R. S.; Jaeger, T. D.; Duncan, M. A. Infrared Spectroscopy of $Ni^+(C_2H_2)_n$ Complexes: Evidence for Intracluster Cyclization Reactions. *J. Phys. Chem. A* **2002,** *106*, 10482-10487.
83. Hewage, D.; Silva, W. R.; Cao, W.; Yang, D.-S. La-Activated Bicyclo-Oligomerization of Acetylene to Naphthalene. *J. Am. Chem. Soc.* **2016,** *138*, 2468−2471.
84. Kumari, S.; Cao, W.; Zhang, Y.; Roudjane, M.; Yang, D.-S. Spectroscopic Characterization of Lanthanum-Mediated Dehydrogenation and C−C Bond Coupling of Ethylene. *J. Phys. Chem. A* **2016,** *120*, 4482−4489.
85. Tsui, E. Y.; Müller, P.; Sadighi, J. P. Reactions of a Stable Monomeric Gold(I) Hydride Complex. *Angew. Chem. Int. Ed.* **2008,** *47*, 8937−8940.

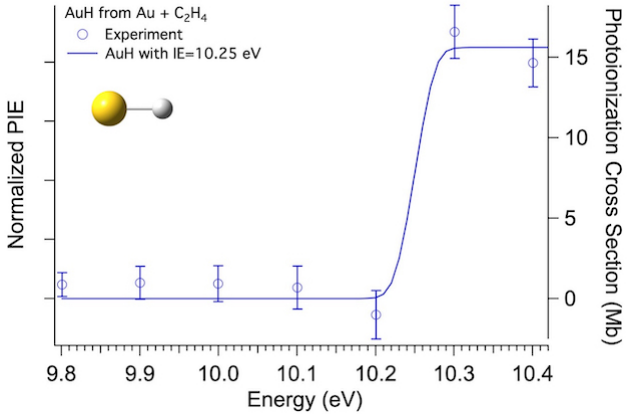
AuH from Au + C_2H_4
Experiment
AuH with IE=10.25 eV
Normalized PIE
Photoionization Cross Section (Mb)
Energy (eV)
9.8
9.9
10.0
10.1
10.2
10.3
10.4
0
5
10
15

TOC figure